

## Effects of Oxygen Ion Irradiation on PZT Modified Ferroelectric Materials for Space Applications

Padmaja Guggillia\*, Ryan Moxon, A. K. Batra and Rachel Powell

Department of Physics, Alabama A&M University, Normal, AL 35762, USA

### \*Corresponding author

Padmaja Guggillia, Department of Physics, Alabama A&M University, Normal, AL 35762, USA, E-mail: padmaja.guggilla@aamu.edu.

Submitted: 28 Nov 2016; Accepted: 07 Dec 2016; Published: 11 Dec 2016

### Abstract

Lead magnesium niobate-lead titanate (PMN-PT) is an important and high performance piezoelectric and pyroelectric relaxor material having wide range of applications in infrared sensor devices. Present work studies the fabrication and dielectric characteristics of PMN-PT in the bulk form. The PMN-PT bulk material was prepared in sol-gel method and subsequently irradiated with heavy ion oxygen. The materials were analyzed and determined that the relaxor ferroelectric material indicated changes in its dielectric constant and pyroelectric coefficient after irradiation. Due to the radiation fluent of  $1 \times 10^{16}$  ions/cm<sup>2</sup>, the dielectric constant of the material increased uniformly, while its pyroelectric coefficient showed a sharp increase to the value of  $5 \times 10^{-9}$   $\mu\text{C}/\text{cm}^2 \text{ } ^\circ\text{C}$  with increase in temperature. Its dielectric constants showed increase in values of  $527 \mu\text{C}/\text{cm}^2 \text{ } ^\circ\text{C}$  at  $50^\circ\text{C}$ ,  $635 \mu\text{C}/\text{cm}^2 \text{ } ^\circ\text{C}$  at  $60^\circ\text{C}$  and  $748 \mu\text{C}/\text{cm}^2 \text{ } ^\circ\text{C}$  at  $70^\circ\text{C}$ . Properties such as the material impedance, admittance and modulus were investigated for changes in properties which became evident after irradiation. In this paper effect of oxygen ion irradiation on the  $\text{LiTaO}_3$  and two commercial samples BM 300 and BM 941 are also reported and analyzed. All these bulk materials were functional even after irradiation and was showing enhancement in some of the key characteristics of ferroelectric material.

**Keywords:** Heavy Ion oxygen; Irradiation; Dielectric Constants; Pyroelectric Coefficient; Admittance; Impedance; Modulus.

### Introduction

Lead magnesium niobate-Lead titanate:  $[\text{Pb}(\text{Mg}_{1/3}\text{Nb}_{2/3})\text{O}_3]_{0.8}\text{-}[\text{PbTiO}_3]_{0.2}$  hereon referred as PMN-PT is a lead based ferroelectric material [1]. BM 300 is a commercial modified PZT ( $\text{Pb}_{1.02}(\text{Zr}_{0.58}\text{Fe}_{0.20}\text{Nb}_{0.22}\text{Ti}_{0.02})$ ) material and will be referred as BM300 here on. BM941 ( $\text{PbNb}_2\text{O}_6$ ) and  $\text{LiTaO}_3$  are two another commercial samples which are characterized for their functionality before and after irradiation. All these materials dielectric constant change slowly in a wide range of temperatures and show strong frequency dispersion. PMN-PT is a good ferroelectric material which possesses superior dielectric and piezoelectric properties. These unique properties make the PMN-PT material ideal candidate for many applications including space applications such as IR sensors and actuators in the radiation environment as well as space [2,3]. Present work examines the functionality and characteristics of bulk PMN-PT in space where there is radiation present. Due to the exposure to the radiation in space, the material possibly undergoes a systematic structural change as a result of induced defects [4]. The mechanism for transfer of energy from the radiation to the material during irradiation is well known. A high energy heavy ion loses its energy in a medium through two processes; electronic loss and nuclear collisions [5]. The

latter process is the dominant mode of energy loss at low ion energies and is responsible for displacing atoms of the medium from their lattice positions [5]. The electronic energy loss is appreciable at higher energy and in this process the target atom is not displaced but only excited or ionized [6]. However, it can lead to displacement of lattice atoms in a cylindrical core along the ion path in insulating materials either through the Columbic explosion or the thermal spike [6,7]. The irradiation also enhances the role of defects in altering material properties. The electron and holes created by irradiation are violently separated and are then trapped at lattice point defects, stoichiometric defects, impurities and at grain boundaries. It is well known that the grain boundaries offer the site for the trapped charges as they offer high resistance to movement of charges. In ferroelectric materials, these trapped charges pin the domains and consequently affect the ferroelectric properties. Some reported response due to the gamma, electron and neutron irradiation on the lead-based ferroelectric compositions [8]. Understanding the effects of heavy ion irradiation on materials is very important if one intends to use the devices containing these material(s), in the radiation environment like in nuclear reactors [9].

In this research, the composite in bulk form which is obtained commercially was prepared using PMN-PT crystalline powder by solution casting method. The composites with volume fraction

ranging from 0.05 to 0.4 were fabricated using hot-press method [6]. It is worthy to indicate that PMN and PT composites in PMN-PT Relaxor were near its morphotropic phase boundary. The morphotropic phase boundary in the PMN-PT is usually located close to the  $x=0.35$  composition [7]. The functional properties of the material depend on its phase composition [7]. The functional properties also depends on the material composition the processing procedure the crystal orientation the compatibility of the functional material with the electrodes, the poling procedure the grain size and the boundary effects imposed by the material system [8-17,20-23]. In addition, the properties of the PMN-PT ferroelectric material can be certainly modified by the additional application of mechanical stress [18,19]. However, piezoelectric properties are maximizing due to the enhancement of polarizability between the energy states of rhombohedral and tetragonal structures of the material. Such material was subjected to high-energy oxygen-ion irradiation, and observable changes in ferroelectric properties were noted, according to the analysis of the graphical results. The primary objective of this research experiment was to observe and determine by calculations, the changes in material properties before and after irradiation with heavy oxygen ion, having fluent of  $1 \times 10^{16}$  ions per centimeter square. Therefore, emphasis was significantly placed on the material properties such as the impedance, admittance and modulus, in addition to the dielectric constants and pyroelectric coefficient. By fabricating composites with different volume fractions and carefully controlling the radiation dosage, the composites were characterized before and after irradiation for structural changes in dielectric and ferroelectric properties.

## Experiment

### Materials

PMN-PT pellets were obtained from commercial material manufacturer Sensor Technology Ltd., Canada which used solgel method to produce the PMN-PT powder. BM 300 and BM 941 samples having 13.75 mm in diameter and 0.9 mm obtained from Sensor Technology Limited, Canada (www.sensortech.ca).

### Methodology

To measure the capacitance and dielectric loss, a QuadTech 1620 LCR bridge was bought, and it was interface to a computer. To measure the capacitance, a shielded sample holder was required, which was designed and fabricated in AAMU Physics Department. The schematic of the set-up is shown in figure 1. The complete set-up includes a QuadTech Model 1920 precision LCR (Inductance, Capacitance, and Resistance) meter, an Agilent 34970A DMM (Digital Multimeter) with a Type K Thermocouple input for temperature measurement, a Barnant Company Model 669 Temperature Control Unit with a Type K Thermocouple input for feedback loop control, a Staco, Inc. Type 3PN1010 Variac for heater power adjustment, and a PC. A sample is placed in a sample holder for capacitance ( $C_p$ ) and dissipation factor ( $\tan\delta$  (D)) at frequencies from 10 Hz to 1 MHz with the applied signal was  $\sim 10$ V/cm at different temperatures (Figure 1). The temperature is increased and the test fixture is allowed to reach isothermal conditions and then another set of measurements is made. The temperature steps are increased in  $10^\circ\text{C}$  increments up

to  $100^\circ\text{C}$ . The dielectric constant constants ( $\epsilon'$ ,  $\epsilon''$ ) were calculated by measuring capacitance and dielectric loss. The relationship between the impedance and admittance of the material is an inverse relation. Since the Impedance is given as,  $Z'=1/Y'$ , where  $Z'$  represents the impedance and  $Y'$  represents the admittance.

$$Z_{eq} = R_{eq} + jX_{eq} \quad (1)$$

Where,  $R_{eq}$  represents the resistive part of the impedance, and  $X_{eq}$  represents the reactive part of the impedance. The reactive part of the impedance is distinguished by the fact that the sinusoidal voltage across the component and is in quadrature with the sinusoidal current through the component. It implies that when the material is used as a capacitor in a circuit, it absorbs energy from the circuit and then returns energy to the circuit. This is unlike a resistance; a reactance does not dissipate power. The expression for the admittance in terms of voltage and current can also be written as;

$$Y=I/V =G + jB, \quad (2)$$

where  $G$  represent the real part of the admittance and  $B$ , the imaginary part of the admittance. Substituting the expression for  $Z=R + jB$  in  $Y=1/Z$  after simplifying and equating to  $G+jB$ , the expressions are

$$G=\text{Re}(Y) = [R/(R^2 + X^2)]^{1/2} \quad (3)$$

$$\text{and } B = \text{Im}(Y) = [X/(R^2 + X^2)]^{1/2} \quad (4)$$

The magnitude of the admittance is given by:

$$|Y| = (G^2 + B^2)^{1/2} = 1/(R^2 + X^2)^{1/2} \quad (5)$$

$$\omega = 2\pi f \text{ where } f \text{ is frequency} \quad (6)$$

$C_s$  and  $C_p$  are series and parallel capacitances respectively.  $M'$  and  $M''$  are real and imaginary parts of modulus.

$$C_s = C_p \times (1 + (\tan \delta)^2) \quad (7)$$

$$Z'' = 1/(\omega \times C_s) \quad (8)$$

$$Z' = Z'' \times \tan \delta \quad (9)$$

$$G_p = Z' / (Z'^2 + Z''^2) \quad (10)$$

$$Y' = G_p \quad (11)$$

$$Y'' = \omega \times C_p \quad (12)$$

$$M' = \omega \times Z' \quad (13)$$

$$M'' = 1/C_s \quad (14)$$

In order to characterize the pyroelectric current measurements, the sample was placed in the sample holder set-up shown above and pyroelectric current  $I_p$  was measured using Byer and Roundy method (Byer, R. L. and Roundy, C. B., 1972), and the pyroelectric coefficient ( $p$ ) was calculated using a relationship:

$$P = \frac{I_p}{A \frac{dT}{dt}} \quad (15)$$

Where  $A$  is the electrode area (identical areas for the opposite electrodes used in each sample), and  $\frac{dT}{dt}$  is the rate of change of temperature. The pyroelectric current is measured using a 6517 Keithley electrometer, and temperature is measured by the HP34970 digital multi-meter using type K thermocouple.

The pyroelectric electrical measurements were conducted before and after the irradiation for BM 300 and BM 941 samples having 13.75 mm in diameter and 0.9 mm. The same procedure was followed for  $\text{LiTaO}_3$  referred as LT here on. The samples were

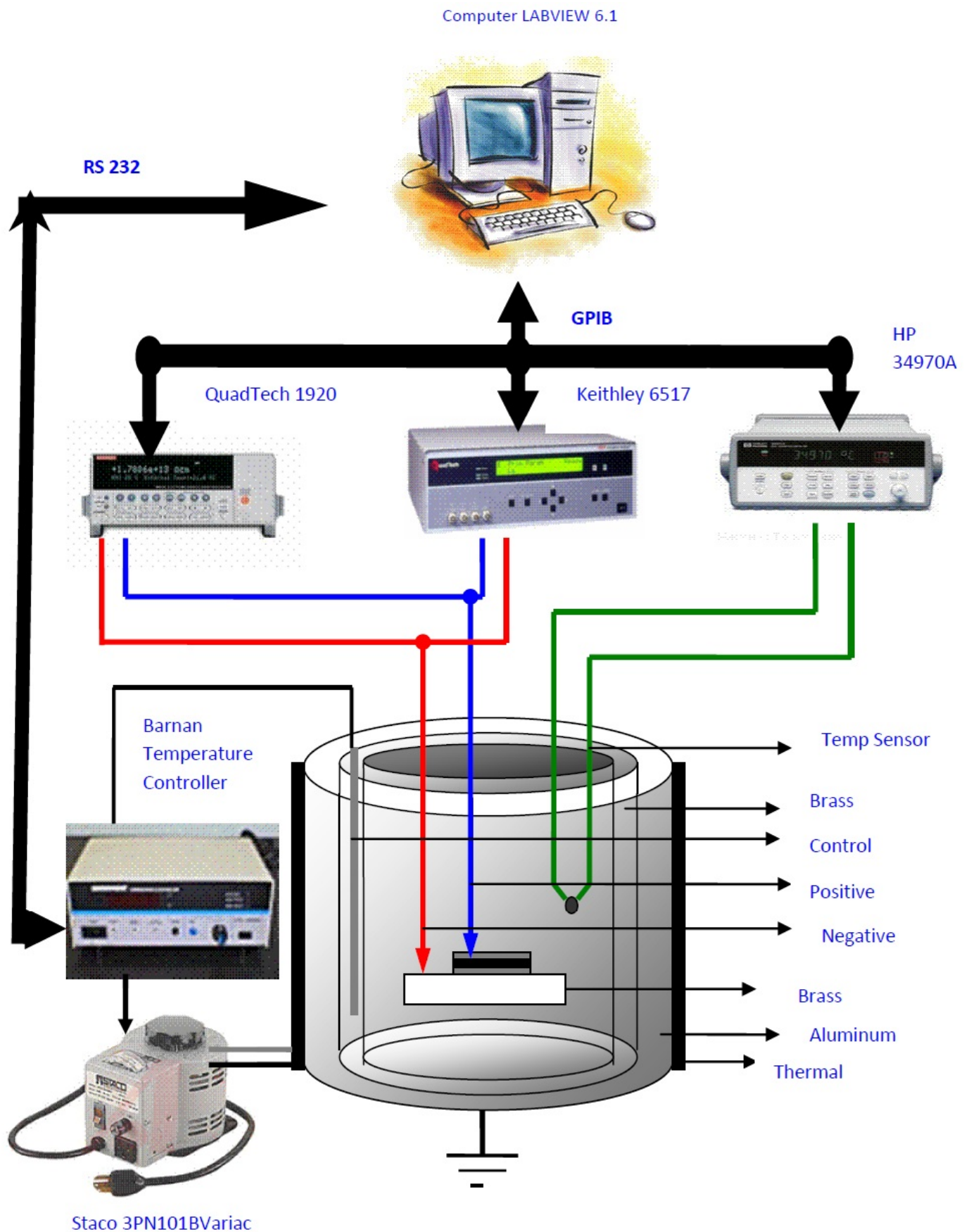


**Figure 1:** A Schematic Diagram of the Dielectric Measurement Set-up.

subjected to irradiation at room temperature by  $O^+$  ions of 200 keV energy using the 2 Megavolt Tandem Model 6SDH-2 National Electrostatics Corporation Pelletron Accelerator at the Leach Science Center of Auburn University, Auburn, AL (USA). The fluence was  $1.0 \times 10^{16}$  ions/cm<sup>2</sup>.

### Results and Discussions

The PMN-PT material does demonstrate an increase in the dielectric constants and dielectric loss with an increase in temperature as shown in figure 2 and also exhibited frequency dispersion behavior of both the dielectric constant and dielectric loss, which is also a characteristic factor or phenomenon of relaxor ferroelectric. According to research performed by other researchers, the Curie temperatures of the PMN-PT tend to increase as the PT powder quantity increase [23].

As shown in figure 3 the dielectric constant and the dielectric loss of PMN-PT after irradiation of heavy oxygen- ion is following the characteristic of the ferroelectric material but the value of the dielectric constant decreased which made material to be better in the applications where less dielectric constant is required.

As is noted from the figures 2 and 3 the dielectric constants for the PMN-PT material before and after oxygen-ion irradiation, the values for the Dielectric Constants at 25°C before irradiation is  $2000 \mu C/cm^2 \text{ } ^\circ C$  and the value for the constant at 25°C after irradiation is  $345 \mu C/cm^2 \text{ } ^\circ C$ .

At 40°C before irradiation, the dielectric constants are  $2450 \mu C/cm^2 \text{ } ^\circ C$ , and the value after irradiation is  $455 \mu C/cm^2 \text{ } ^\circ C$ . At 60°C before irradiation, the dielectric constant is  $3190 \mu C/cm^2 \text{ } ^\circ C$ , and the value after irradiation is  $645 \mu C/cm^2 \text{ } ^\circ C$ . In this aspect, the conductivity of the material before irradiation is higher that it's conductivity after irradiation. After irradiation, the material's capacitance will also decrease. Since Capacitance is  $C = \epsilon \epsilon_0 \epsilon' d/A$ , where d represents the thickness of the material and A represents the surface area of the sample. Such decreased in dielectric coefficient after irradiation is attributed to the structural defects instituted in the material due to the heavy bombardment of the oxygen-ion irradiation.

Figures 4-6 show the dependency of the impedance, admittance and modulus on temperature. Impedance of the PMN-PT decreases with temperature and since admittance is opposite of impedance it increases with increase in the temperature. Modulus of the PMN-PT also decreases with increase in temperature.

As noted from the graphs the Dielectric Constants at 25°C before irradiation is  $2000 \mu C/cm^2 \text{ } ^\circ C$  and the value for the constant at 25°C after irradiation is  $345 \mu C/cm^2 \text{ } ^\circ C$ . At 40°C before irradiation, the dielectric constants are  $2450 \mu C/cm^2 \text{ } ^\circ C$ , and the value after irradiation is  $455 \mu C/cm^2 \text{ } ^\circ C$ . At 60°C before irradiation, the dielectric constant is  $3190 \mu C/cm^2 \text{ } ^\circ C$ , and the value after irradiation is  $645 \mu C/cm^2 \text{ } ^\circ C$ . According to these graphical results, it has been established that the dielectric constants of the PMN-PT ferroelectric material showed a significant decreased in value after oxygen-ion irradiation. In this aspect, the conductivity of

the material before irradiation is higher that it's conductivity after irradiation.

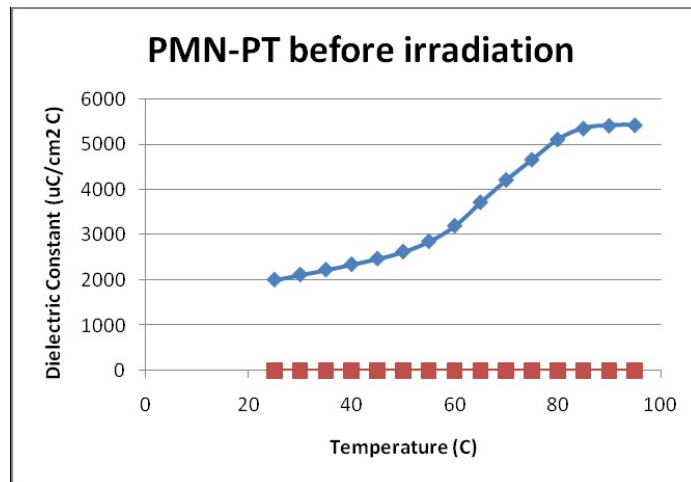


Figure 2: Real & Imaginary Part of Dielectric Constant Vs Temperature.

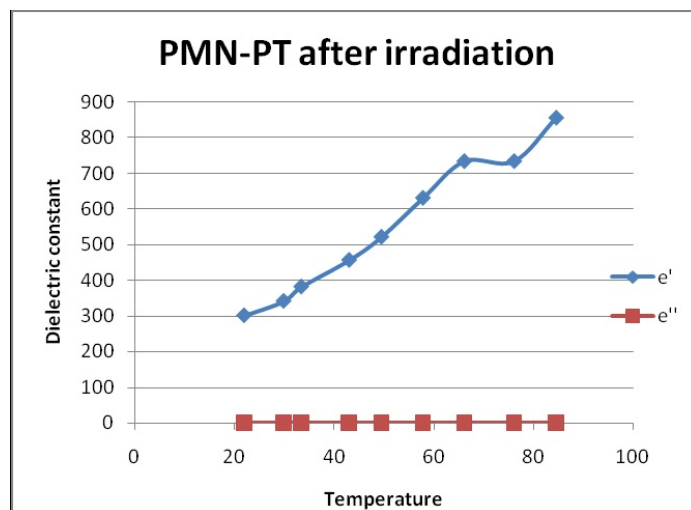


Figure 3: Dielectric Constant Vs Temperature of After Oxygen- ion Irradiation.

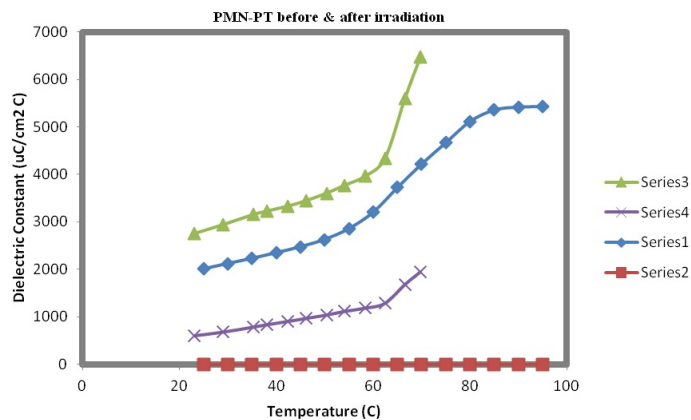


Figure 4: Comparison of Real & Imaginary Part of Dielectric Constants Before and After Irradiation.

This conclusion is based on the formula for AC conductivity of the material which is:

$$\sigma AC = \omega \epsilon_0 \epsilon' \tan(\delta) \quad (15)$$

Where;  $\omega$  represents the radiating frequency,  $\epsilon_0$  represents the permittivity of free-space, having value of: ( $\epsilon_0=8.854 \times 10^{-12} \text{F/m}$ );  $\epsilon'$  is the real part of the dielectric constant of the material, and is also known as the Fresnel reflection coefficient.  $\tan(\delta)$  is the ratio of the real part of the dielectric constant to the imaginary part of the dielectric constant, which is,  $\epsilon''/\epsilon'$ . The imaginary part of the dielectric constant will give the radio absorption coefficient.

After irradiation, the material's capacitance will also decrease. Since the mathematical formula for the Capacitance is  $C=\epsilon_0 \epsilon' d/A$ , where  $d$  represents the thickness of the material and  $A$  represents the surface area of the sample. Such decreased in dielectric coefficient after irradiation is attributed to the structural defects instituted in the material due to the heavy bombardment of the oxygen-ion irradiation. In accordance to the graph above, the dielectric constant for the PMN-PT material showed an increased in dielectric constant after the oxygen-ion irradiation. However, at room temperature of 25°C, the dielectric constant is 1890 $\mu\text{C}/\text{cm}^2$  °C and after the irradiation for the same temperature, the value of the dielectric constant is 2875 $\mu\text{C}/\text{cm}^2$  °C.

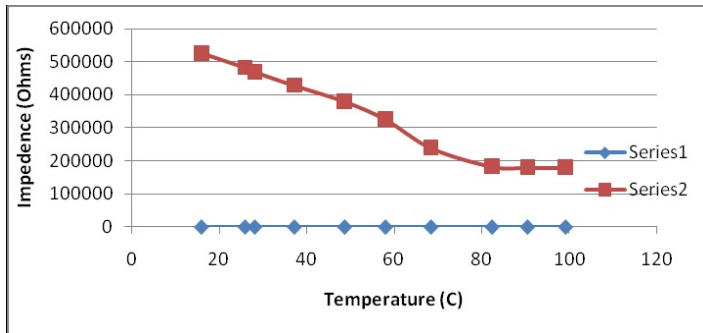


Figure 5: PMN-PT Impedance before Irradiation.

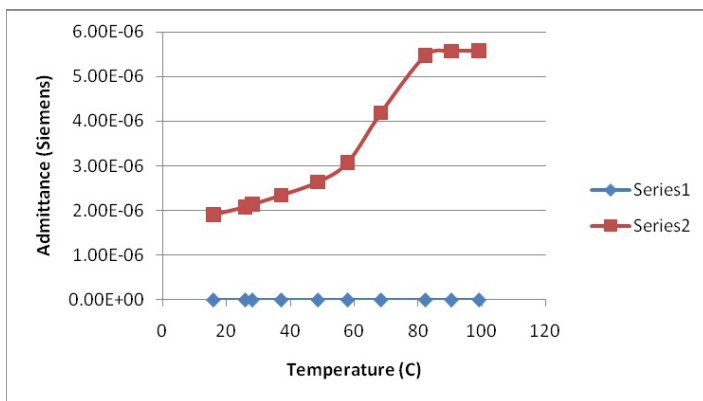


Figure 6: PMN-PT Admittance before Irradiation.

After irradiation with the heavy oxygen-ion, impedance of PMN-PT decreased in the value but followed the same tendency of increment with an increment in temperature.  $Z'$  values of PMN-PT after irradiation decreased about an order of 10 and  $Z''$  increased at an order of 10 after irradiation with Oxygen ion. With the increase in impedance, the material is rendered to a high resistance to the electric flow of charge. The dielectric constant of the material will reach a peak as its temperature increase and subsequently begins

to drop as the temperature continues to increase. The dielectric constant as a function of temperature will display such phenomena.

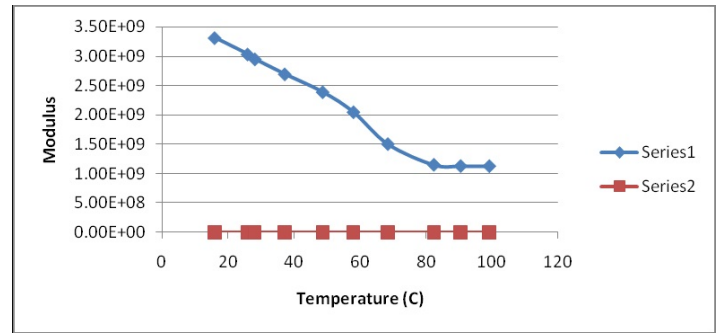


Figure 7: PMN-PT Modulus before Irradiation.

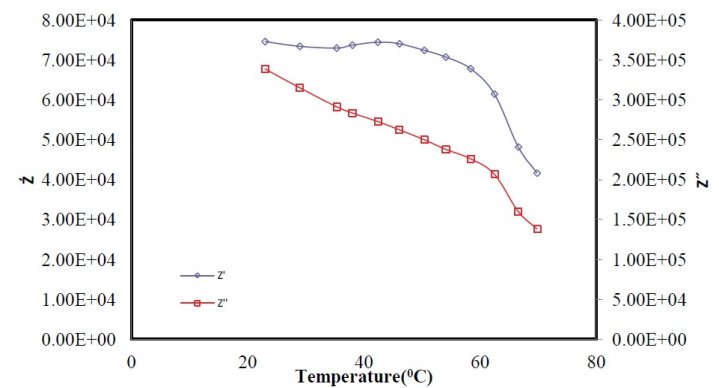


Figure 8: Impedance value for PMN-PT after Oxygen-ion Irradiation.

Figure 8 shows the increase the impedance of both real and imaginary parts of PMN-PT with increment in temperature but after irradiation the value of the admittance decreases compared to before irradiation. As impedance and admittance are reverse of each other even after the irradiation PMN-PT follows the basic material property. Figure 10 shows the variation of modulus with variation in temperature and this phenomenon is attributed to the phase shift. The electric modulus formalism  $M'$  and  $M''$  is proportional to the inverse of the  $\epsilon''$ .

Although it was originally introduced by Macedo to study space charge relaxation phenomena, Modulus representation is now widely used to analyze ionic conductivities. Generally, for a pure conduction process, a relaxation peak would be observed in the frequency spectra of the imaginary component  $M''$  and no peak would take place in the corresponding plot of  $\epsilon''$ . However, piezoelectric properties are maximized due to the enhancement of polarizability between the energy states of given to the material properties such as its dielectric constant, pyroelectric coefficient, Admittance, Impedance and Modulus. After irradiating the PMN-PT with heavy-ion oxygen, the material possesses a low value of the impedance because the capacitance after irradiation is also assumed to be low. The impedance can be defined by the ratio of two phasors where a phasor is complex peak amplitude of a sinusoidal function of time. After irradiation, the dielectric constants for most of the materials showed a decreased in value, which means that the Conductivity and capacitance will also decrease after irradiation.

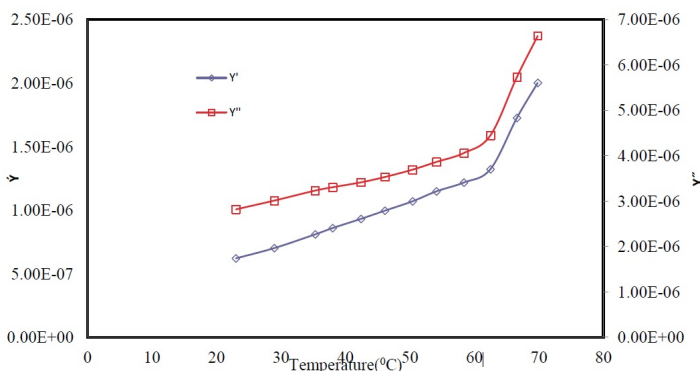


Figure 9: Admittance of PMN-PT after Oxygen-ion Irradiation.

Impedance and admittance are inversely proportional to each other and the impedance of the circuit element is the ratio of the phasor voltage across the element to the phasor current through the element. Although  $Z$  is the ratio of two phasors,  $Z$  is not a phasor itself. That is,  $Z$  is not associated with some sinusoidal function of time. Before irradiation, the dielectric constants of the materials showed an increase in dielectric properties up to a critical temperature and then it begins to decrease as the temperature increases which is a phenomena associated with the ferroelectric materials.

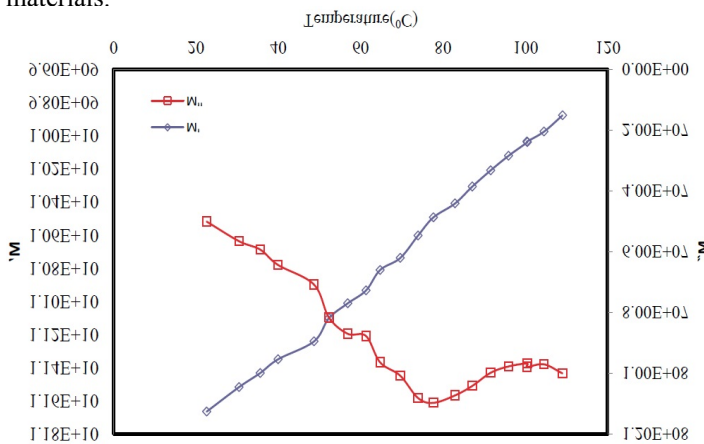


Figure 10: Modulus of PMN-PT after oxygen-ion irradiation.

BM 300 material which is a modified lead titanate compositions offering great flexibility in transducer design due to a very high anisotropy in piezoelectric properties. This ceramic in Figure 10 can be used in applications where interference from radial modes is a significant problem. The principal features of the ceramic are its high Curie temperature of 225°C, a relatively low dielectric constant of  $-1.5\mu\text{C}/\text{cm}^2\text{K}$ , a high anisotropy of electromechanical coupling coefficient, high relative dielectric constant of 200, a coupling factor of 0.05, mechanical quality factor of 800, density of  $6.7\text{g}/\text{cm}^2$ . The material has good mechanical properties and low ageing characteristics.

Tables 1-4 give the details of the pyroelectric characteristics of BM 300, BM941, LT and PMN-PT before and after irradiation. From these tables it is evident that all the materials were functional after irradiation and have all the pyroelectric properties are enhanced to

some extent which is attributed to the defects in material structure created due to the heavy oxygen ion bombardment during irradiation.

Temp	BM 300 Before Irradiation			BM300 After Irradiation		
	50°C	60°C	70°C	50°C	60°C	70°C
$\rho$	$2 \times 10^{-8}$	$3 \times 10^{-8}$	$310^{-8}$	$6 \times 10^{-8}$	$8 \times 10^{-8}$	$1.2 \times 10^{-8}$
$\epsilon'$	203.51	210.59	222.11	65	67.8	72
$\epsilon''$	4.3385	5.3915	7.2598	2.34	3.37	3.77
$Z'$	863	915	993	$5 \times 10+3$	$7 \times 10+3$	$8 \times 10+3$
$A'$	$2 \times 10^{-7}$	$5 \times 10^{-7}$	$5 \times 10^{-7}$	$7 \times 10^{-8}$	$12 \times 10^{-8}$	$14 \times 10^{-8}$
$M'$	$1 \times 10^{-7}$	$2 \times 10^{-7}$	$4 \times 10^{-7}$	$2 \times 10^{-9}$	$1 \times 10^{-9}$	$1 \times 10^{-9}$

Table 1: Pyroelectric Properties of BM 300 before and After Irradiation.

Temp	BM 941 Before Irradiation			BM941 After Irradiation		
	50°C	60°C	70°C	50°C	60°C	70°C
$\rho$	$8.0 \times 10^{-9}$	$9.1 \times 10^{-8}$	$1.2 \times 10^{-8}$	$1.3 \times 10^{-8}$	$2.2 \times 10^{-8}$	$2.5 \times 10^{-8}$
$\epsilon'$	739.94	756.64	774.65	24.4	24.9	25.3
$\epsilon''$	9.9337	11.380	11.247	0.43	0.46	0.48
$Z'$	$262 \times 10+3$	$278 \times 10+3$	$291 \times 10+3$	$8.0 \times 10+3$	$9.3 \times 10+3$	$13.2 \times 10+3$
$A'$	$4.0 \times 10^{-8}$	$4.6 \times 10^{-8}$	$5.6 \times 10^{-8}$	$1.6 \times 10^{-8}$	$2.3 \times 10^{-8}$	$2.5 \times 10^{-8}$
$M'$	$4.5 \times 10^{-9}$	$4.4 \times 10^{-9}$	$4.3 \times 10^{-9}$	$4.5 \times 10^{-9}$	$4.3 \times 10^{-9}$	$4.3 \times 10^{-9}$

Table 2: Pyroelectric Properties of BM 941 before and After Irradiation.

Temp	LT Before Irradiation			LT After Irradiation		
	50°C	60°C	70°C	50°C	60°C	70°C
$\rho$	$1.4 \times 10^{-8}$	$1.6 \times 10^{-8}$	$1.8 \times 10^{-8}$	$4.0 \times 10^{-8}$	$4.8 \times 10^{-8}$	$4.8 \times 10^{-8}$
$\epsilon'$	582.37	592.93	604.48	62.1	64.2	65.2
$\epsilon''$	$5.5 \times 10^{-8}$	$5.7 \times 10^{-8}$	$6 \times 10^{-8}$	0.05	0.07	0.08
$Z'$	263	291	383	$1.1 \times 10^{-4}$	$1.3 \times 10^{-4}$	$1.5 \times 10^{-4}$
$A'$	$4.0 \times 10^{-9}$	$8.0 \times 10^{-8}$	$9 \times 10^{-8}$	$3.3 \times 10^{-9}$	$4.5 \times 10^{-9}$	$5.4 \times 10^{-9}$
$M'$	$1.4 \times 10^{-9}$	$1.2 \times 10^{-9}$	$1 \times 10^{-8}$	$1.1 \times 10^{+10}$	$1.1 \times 10^{+10}$	$1.1 \times 10^{+10}$

Table 3: Pyroelectric Properties of LT before and After Irradiation.

Temp	PMN-PT Before Irradiation			PMN-PT After Irradiation		
	50°C	60°C	70°C	50°C	60°C	70°C
$\rho$	$2.5 \times 10^{-8}$	$3.9 \times 10^{-8}$	$5.4 \times 10^{-8}$	$1.5 \times 10^{-8}$	$1.61 \times 10^{-8}$	$1.8 \times 10^{-8}$
$\epsilon'$	183	192	198	527	635	748
$\epsilon''$	6.50	7.83	8.42	6.3	6.72	6.84
$Z'$	$6.3 \times 10+3$	$7.1 \times 10+3$	$8.2 \times 10+3$	$7.3 \times 10+4$	$6.4 \times 10+4$	$4.1 \times 10+4$
$A'$	$8.0 \times 10^{-8}$	$12.0 \times 10^{-8}$	$18.4 \times 10^{-8}$	$1.1 \times 10^{-6}$	$1.3 \times 10^{-6}$	$1.6 \times 10^{-6}$
$M'$	$3.0 \times 10^{-9}$	$2.93 \times 10^{-9}$	$2.9 \times 10^{-9}$	$15.2 \times 10^{-8}$	$14.0 \times 10^{-8}$	$7.0 \times 10^{-8}$

Table 4: Pyroelectric Properties of PMN-PT before and After Irradiation.

## Conclusions

The experiment of effects of Oxygen ion irradiation on PMN-PT, BM300, BM941, and LT bulk materials for space applications proved successful as the material was functional even after the heavy

Oxygen ion irradiation. The bulk materials were characterized for their dielectric, impedance, admittance and modulus properties to determine the functionality of the material in space environment. The calculated dielectric, impedance, admittance and modulus values were dependent on temperature variations which are a key characteristic of ferroelectric materials.

### Acknowledgment

This work has been supported DHS-BS Award #2010-ST-062-000034.

### References

1. Chen J, Shurland A, Perry J, Chamann B, RGururara T (1996) Process of the 10th IEEE International Symposium on Application of Ferroelectric 27-32.
2. Yin QR, Fang JW, Luo HS, Li GR (2000) Processing of the 12th IEEE International Symposium on Application of Ferroelectric, Honolulu, Hawaii, USA, July 569-572.
3. Das-Gupta DK Zhang S (1992) Non polar polymer/ferro and antiferroelectric ceramic composite films for high energy storage applications, *Ferroelectrics* 134: 71-77.
4. Sun W, Lu B (2006) Characterisation of proton-irradiated 65PMN–35PT/P(VDF–TrFE) 0–3 composites. *Materials Science and Engineering B* 127: 144-149.
5. Zhang QM, Bharathi V, Zhao X (1998) Giant electrostriction and relaxor ferroelectric behaviour in electron-irradiated poly (vinylidene fluoride-trifluoroethylene) copolymer, *Science* 280: 2101-2103.
6. Batra AK, Aggarwal MD, Matthew Edwards, Amar Bhalla (2007) Ferroelectric- Present Status of Polymer Ceramic Composites for pyroelectric Infrared detectors 114.
7. Hana Ursic, Marina Santo Zarnick, Marija Kosec (2011) Pb (Mg<sub>1/3</sub>Nb<sub>2/3</sub>) O<sub>3</sub>.PbTiO<sub>3</sub> (PMN-PT) Material for Actuator Applications. *Smart Materials Research* 1.
8. Kelly J, Leonard M, Tantigate C, Safari A (1997) Effects of composition on the electromechanical properties of (1-x) Pb (Mg<sub>1/3</sub>Nb<sub>2/3</sub>)O<sub>3-x</sub> PbTiO<sub>3</sub> ceramics. *Journal of the American Ceramic Society* 80: 957-964.
9. Alguero M, Moure A, Pardo L, Hole J, Kosec M (2006) Processing by mechanosynthesis and properties of piezoelectric Pb (Mg<sub>1/3</sub>Nb<sub>2/3</sub>)O<sub>3</sub>.PbTiO<sub>3</sub> with different compositions. *Acta Materials* 54: 501-511.
10. Leite ER, Scotch AM, Khan A, Tao Li, Helen M, et al. (2002) Chemical heterogeneity in PMN-PT ceramic and effects on the dielectric and piezoelectric properties. *Journal of the American Ceramic Society* 85: 3018-3024.
11. Zhang R, Jiang B, Cao W (2001) Elastic, piezoelectric, and dielectric properties of multidomain 0.67Pb (Mg<sub>1/3</sub>Nb<sub>2/3</sub>)O<sub>3</sub>.0.33PbTiO<sub>3</sub> single crystals. *Journal of Applied Physics* 90: 3471-3475.
12. Zhang R, Jiana B, Cao W (2003) Orientation dependence of piezoelectric properties of single crystals domain 0.67Pb (1-x)[Pb(Mg<sub>1/3</sub>Nb<sub>2/3</sub>)O<sub>3</sub>.0.33PbTiO<sub>3</sub> crystals. *Applied Physics lecture* 82: 3737-3739.
13. Ursic H, Tellier J, Hrovat M, Holc J, Drnovšek S, et al. (2011) The effects of poling on the properties of 0.65Pb (Mg<sub>1/3</sub>Nb<sub>2/3</sub>) O<sub>3</sub>.0.35PbTiO<sub>3</sub> Ceramics. *Japanese Journal of Applied Physics* 50.
14. Guo Y, Luo H, Chen K, Xu H, Zhang X, et al. (2002) Effects of Composition and poling field on the properties and ferroelectric phase – stability of Pb (1-x)[Pb(Mg<sub>1/3</sub>Nb<sub>2/3</sub>)O<sub>3</sub>.PbTiO<sub>3</sub> crystals. *Journal of Applied Physics* 92: 6134-6138.
15. Alguero M, Ricote J, Jimenez R, Ramos P, Carreaud J, et al. (2007) Size effects in morphotropic phase boundary Pb (Mg<sub>1/3</sub>Nb<sub>2/3</sub>)O<sub>3</sub>.PbTiO<sub>3</sub>. *Applied physics lecture* 91: 11.
16. Carreaud J, Gemeiner P, Kiat JM (2005) Size driven relaxation and polar states in Pbm<sub>1/3</sub>Nb<sub>2/3</sub>O<sub>3</sub>-based system. *Physical Review* 72: 1-6.
17. Alguero M, Jimenez B, Pardo L (2005) Transition between the relaxor and ferroelectric states for (1-x)Pb[Mg<sub>1/3</sub>Nb<sub>2/3</sub>] O<sub>3-x</sub>PbTiO<sub>3</sub> with x=0.2 and x=0.3 polycrystalline aggregates. *Applied Physics lecture* 87: 3.
18. Lefki K, Dormans GJM (2005) Measurements of piezoelectric Coefficients of ferroelectric thin film. *Journal of Applied Physics* 98: 5.
19. Wan Q, Chen C, Shen YP (2005) Effects of Stress and electric field on the electromechanical properties of Pb(1-x) [Pb(Mg<sub>1/3</sub>Nb<sub>2/3</sub>)O<sub>3</sub>.0.32PbTiO<sub>3</sub> Single Crystal. *Journal of Applied Physics* 98: 5.
20. Ursic H, Hrouat M, Hole J, (2010) Influence of the substrate on the phase composition and electrical properties of 0.65PMN-0.35PT thick film. *Journal of European Ceramic Society* 30: 2081-2092.
21. Ursic H, Zarnik MS, Tellier J, Hrovat M, Hole J, et al. (2014) The influence of thermal stress on the phase composition of 0.65Pb(1-x).
22. Kubo R (1957) Statistical-Mechanical Theory of Irreversible Processes. I. General Theory and Simple Applications to Magnetic and Conduction Problems. *J Phys Soc Japan* 12: 570-586.
23. Roling B (1999) What do electrical conductivity and electrical modulus spectra tell us about the mechanisms of ion transport processes in melts, glasses, and crystals? *Journal of Non-Crystalline Solids* 244: 34-43.

**Copyright:** ©2016 Padmaja G, et al. This is an open-access article distributed under the terms of the Creative Commons Attribution License, which permits unrestricted use, distribution, and reproduction in any medium, provided the original author and source are credited.